Biophys Rep 2020, 6(6):278–289
https://doi.org/10.1007/s41048-020-00120-z

Biophysics Reports

RESEARCH ARTICLE

Amphiphilic peptide dendrimer-based nanovehicles for safe and effective siRNA delivery

Chi Ma[1], Dandan Zhu[1], Yu Chen[1], Yiwen Dong[1], Wenyi Lin[1], Ning Li[1], Wenjie Zhang[1], Xiaoxuan Liu[1]✉

[1] State Key Laboratory of Natural Medicines and Jiangsu Key Laboratory of Drug Discovery for Metabolic Diseases, Center of Advanced Pharmaceuticals and Biomaterials, China Pharmaceutical University, Nanjing 210009, China

Received: 28 July 2020 / Accepted: 18 September 2020 / Published online: 21 November 2020

Abstract Small interfering RNA (siRNA)-based RNA interference has emerged as a promising therapeutic strategy for the treatment of a wide range of incurable diseases. However, the safe and effective delivery of siRNA therapeutics into the interior of target cells remains challenging. Here, we disclosed novel amphiphilic peptide dendrimers (AmPDs) that composed of hydrophobic two lipid-like alkyl chains and hydrophilic poly(lysine) dendrons with different generations ($2C_{18}$-KK_2 and $2C_{18}$-KK_2K_4) as nanovehicles for siRNA delivery. These AmPDs are able to self-assemble into supramolecular nanoassemblies that are capable of entrapping siRNA molecules into nanoparticles to protect siRNA from enzymatic degradation and promote efficient intracellular uptake without evident toxicity. Interestingly, by virtue of the optimal balance of hydrophobic lipid-like entity and hydrophilic poly(lysine) dendron generations, AmPD $2C_{18}$-KK_2K_4 bearing bigger hydrophilic dendron can package siRNA to form stable, but more ready to disassemble complexes, thereby resulting in more efficient siRNA releasing and better gene silencing effect in comparison with AmPD $2C_{18}$-KK_2 bearing smaller dendron. Additional studies confirmed that $2C_{18}$-KK_2K_4 can capitalize on the advantages of lipid and peptide dendrimer vectors for effective siRNA delivery. Collectively, our AmPD-based nanocarriers indeed represent a safe and effective siRNA delivery system. Our findings also provide a new perspective on the modulation of self-assembly amphiphilic peptide dendrimers for the functional and adaptive delivery of siRNA therapeutics.

Keywords Amphiphilic peptide dendrimer, Supramolecular nanoassemblies, RNA interference, siRNA delivery

INTRODUCTION

Small interfering RNA (siRNA), a double-stranded RNA molecule with 19–23 nucleotides, has the powerful capacity to silence the expression of any gene, such as disease-linked genes, with complementary mRNA sequence via Watson–Crick base pairing (Bajan and Hutvagner 2020; Castanotto and Rossi 2009; Weng *et al*. 2019). SiRNA-based RNA interference (RNAi) (Castanotto and Rossi 2009; Kay 2015; Setten *et al*. 2019; Wittrup and Lieberman 2015) is exploited as a promising therapeutic modality for the treatment of both genetic and acquired diseases, particularly culminating with the approval of siRNA therapeutics Patisiran® and Givosiran® (Ledford 2018; Mullard 2020) by the USA Food and Drug Administration (FDA) and European Commission (EC). Although very promising, the clinical implementation of siRNA therapeutics has been impeded by the poor druggability of naked siRNA

Chi Ma and Dandan Zhu have contributed equally to this work.

Electronic supplementary material The online version of this article (https://doi.org/10.1007/s41048-020-00120-z) contains supplementary material, which is available to authorized users.

✉ Correspondence: xiaoxuanliu@cpu.edu.cn (X. Liu)

molecules resulted from their relatively large molecular weight (~13 kDa), polyanionic and hydrophilic nature, as well as their vulnerability to nuclease degradation (Juliano 2016; Kanasty *et al*. 2013; Whitehead *et al*. 2009) and clearance. Therefore, the development of siRNA-based drugs relies on the exploitation of safe and effective delivery vehicles to deliver siRNA molecules to the cytoplasm of the target cell.

To date, myriad delivery systems have been developed for efficient transportation of siRNA therapeutics (Mullard 2020; Yin *et al*. 2014). Cationic lipids and polymer are the two most advanced representatives (Li *et al*. 2018; Ozpolat *et al*. 2014; Wagner 2012; Wu *et al*. 2017). They are able to form stable complexes with siRNA via electrostatic interactions, protect it from enzymatic degradation, and promote cellular uptake of siRNA. Dendrimers, a special class of synthetic polymers, have emerged as extremely appealing siRNA delivery vehicles by virtue of their precisely defined dendritic structures and unique multivalent features (Kesharwani *et al*. 2014; Khandare *et al*. 2012; Lee *et al*. 2005; Mintzer and Grinstaff 2011; Svenson and Tomalia 2005). In particular, amphiphilic dendrimers married the characteristics of dendrimers and the self-assembling feature of lipids, hence taking the advantages of both dendrimers and lipids carriers for excellent performance on the transportation of siRNA therapeutics (Chen *et al*. 2016; Dong *et al*. 2018; Liu *et al*. 2014, 2015, 2016; Percec *et al*. 2010; Yu *et al*. 2012).

The success of amphiphilic dendrimer-based delivery systems has encouraged further exploitation of their diversity. Peptide dendrimers are type of dendrimers composed of amino acids in branch fashion and hold great potentials for biomedical applications by virtue of their unique properties such as protein-mimic structural features, good biocompatibility, and high resistance to proteolytic digestion (Bracci *et al*. 2003; Crespo *et al*. 2005; Darbre and Reymond 2006; Sadler and Tam 2002; Sapra *et al*. 2019). Novel-designed amphiphilic dendrimers featuring peptide dendrimers as hydrophilic heads are expected to show suitable flexibility, good safety profile, and protein-like properties; therefore, they are of particular interest for siRNA delivery (Dong *et al*. 2020; Heitz *et al*. 2019; Inoue *et al*. 2008; Malhotra *et al*. 2012).

Herein, we reported a new class of amphiphilic peptide dendrimers (AmPDs) for siRNA delivery (Fig. 1). Our previous results have demonstrated that the length of lipid chain in the structure of amphiphilic dendrimers plays a very important role in their self-assembly and their capacity for siRNA delivery (Chen *et al*. 2016). In the present study, we designed the AmPDs-embedded two lipid-like alkyl chains with different generations of hydrophilic poly(lysine) dendrons ($2C_{18}$-KK_2 and $2C_{18}$-KK_2K_4) (Fig. 1A) to gain the more insightful understanding that how the generations of hydrophilic dendron entities of the AmPDs influence their ability for siRNA delivery. We performed systematical investigation on the self-assembling behavior, the secondary structures, siRNA binding ability, and siRNA delivery performance of these two AmPDs. We expected to disclose the rationale behind their different performance on siRNA delivery, thereby providing a new perspective on the modulation of self-assembly amphiphilic peptide dendrimers for safe and effective siRNA delivery.

RESULTS AND DISCUSSION

Robust and reliable synthesis of AmPDs and their physicochemical properties

The structure of amphiphilic peptide dendrimers bearing double C_{18} alkyl chains and poly(lysine) dendrons with different generations is shown in Fig. 1A and the detailed synthesis procedures are described in supplementary materials. In brief, hydrophobic double C_{18} alkyl chains and poly(lysine) dendron (KK_2) were synthesized as described previously (Liu *et al*. 2014; Luo *et al*. 2012). Thereafter, the hydrophobic part was successfully covalent connected with hydrophilic poly(lysine) dendron via Cu(I)-catalyzed azide-alkyne cycloaddition (CuAAC) click reaction to achieve AmPD $2C_{18}$-KK_2. Then AmPD $2C_{18}$-KK_2 was coupled with the protected lysine (Boc-Lys-Boc-OH) and followed the deprotection of Boc to obtain AmPD $2C_{18}$-KK_2K_4 (supplementary Scheme S1). These newly synthesized AmPDs were characterized by ^{1}H-NMR and MS spectrums (Data are shown in supplementary materials).

Next, we assessed the self-assembly behavior of AmPDs in aqueous solution. We first determined the critical aggregation concentration (CAC) of AmPDs using the hydrophobic fluorescent probe Nile Red. As shown in Fig. 2A, the determined CAC values of $2C_{18}$-KK_2 and $2C_{18}$-KK_2K_4 were 8.3 and 10.4 μmol/L, respectively, confirming that $2C_{18}$-KK_2 and $2C_{18}$-KK_2K_4 have the similar self-assembly capacity. And the measurements by dynamic light scattering (DLS) and transmission electron microscopy (TEM) showed that the assemblies formed by AmPDs were spherical and ~200 nm in diameter (Fig. 2B and C). TEM images further revealed the vesicle-like structures formed by the self-assembly of AmPDs in water (Fig. 2C). The zeta potential values of the nanostructures formed by $2C_{18}$-KK_2 and $2C_{18}$-KK_2K_4 were +29.5 mV and +24.1 mV, respectively (Table 1), indicating that the colloidal state of these

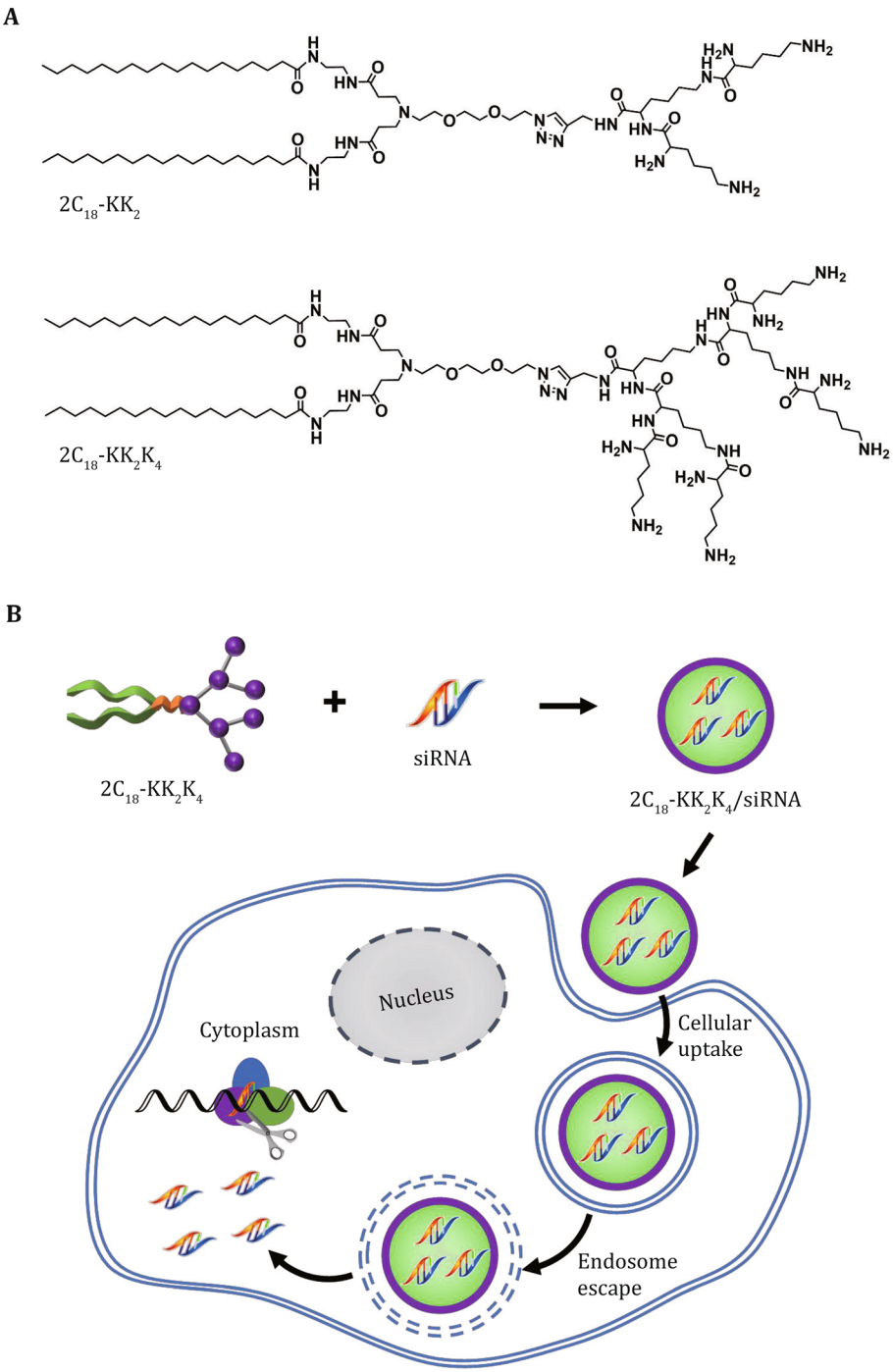

Fig. 1 Graphic illustration of amphiphilic peptide dendrimers (AmPDs)-based supramolecular nanoassemblies for siRNA delivery. **A** Chemical structure of the AmPDs. **B** Cartoon illustration of AmPDs-mediated siRNA delivery

nanoassemblies was stable. All the above results confirmed that the AmPDs ($2C_{18}$-KK_2 and $2C_{18}$-KK_2K_4) could combine the self-assembling characteristics of lipids with the stability and mechanical strength of dendrimer to form stable nanoassemblies in water.

Furthermore, we examined the secondary configurations of these AmPDs using circular dichroism (CD) analysis. The CD spectra of the AmPDs (Fig. 2D) together with their analysis data calculated by CDNN software (Table 1) demonstrated the presence of the secondary structure, implying that the AmPDs retain the protein-mimic features of peptide dendrimers.

Stable formation of siRNA/AmPDs nanoparticles for efficient cellular uptake

The ability of nanocarriers to entrap siRNA to form stable complexes plays a very important role for efficient siRNA delivery, as the so-formed complexes can protect siRNA from enzymatic degradation and facilitate

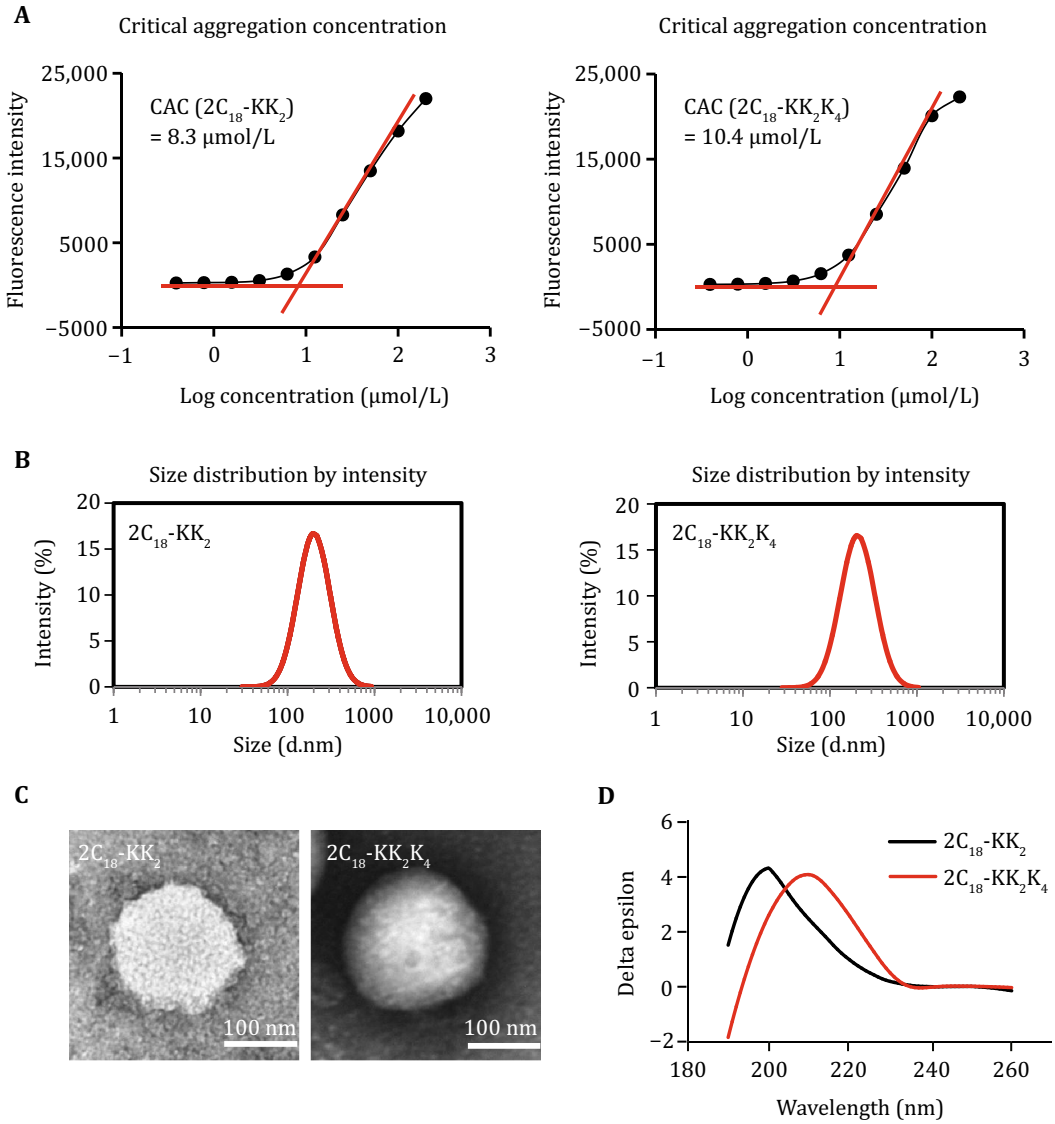

Fig. 2 Characteristics of the AmPDs. **A** The CAC measurements of $2C_{18}$-KK_2 and $2C_{18}$-KK_2K_4 using fluorescent probe Nile Red. **B**, **C** DLS analysis (**B**) and TEM images (**C**) of the $2C_{18}$-KK_2 and $2C_{18}$-KK_2K_4. **D** CD spectrum of AmPDs at concentrations of 0.50 mg/mL in H_2O

Table 1 Physical properties of AmPDs and siRNA/AmPDs

	Diam (nm)	PDI[a]	Zeta potential (mV)	α-heilx (%)	Parallel (%)	β-turn (%)	Rndm. Coil (%)
$2C_{18}$-KK_2	182	0.213	29.5 ± 0.5	12.7	30.4	13.9	43.0
$2C_{18}$-KK_2K_4	189	0.282	24.1 ± 2.5	8.0	41.6	13.0	37.3
siRNA/$2C_{18}$-KK_2	50	0.221	12.1 ± 0.5	27.3	14.9	14.1	43.5
siRNA/$2C_{18}$-KK_2K_4	67	0.315	15.4 ± 1.4	30.0	14.1	14.3	41.6

[a]Polydispersity index

efficient cell uptake (Kim *et al*. 2019). Hence, we first studied the capacity of AmPDs for siRNA entrapment using a gel shift assay (Fig. 3A). Results of RNA migration in gel electrophoresis showed that both $2C_{18}$-KK_2 and $2C_{18}$-KK_2K_4 could entrap and completely retard the migration of siRNA at an N/P ratio $\geq$5.0 (N/P ratio = Total terminal amines in AmPD/phosphates in siRNA). And the so-formed complexes could protect siRNA from RNase digestion (Fig. 3B). We then examined the size and morphology of the siRNA/AmPDs complexes using TEM and DLS. The TEM images revealed that the resulting siRNA/AmPDs complexes were spherical nanoparticles with about 50 nm in size (Fig. 3C). Additional DLS analysis showed that the average size of siRNA/$2C_{18}$-KK_2 complexes was 50 nm with PDI 0.221, while that of siRNA/$2C_{18}$-KK_2K_4 complexes was 67 nm with PDI 0.315 (Fig. 3D; Table 1), which correlated well with the observations in TEM. The surface charges of siRNA/$2C_{18}$-KK_2 and siRNA/$2C_{18}$-KK_2K_4 complexes were characterized by zeta potential of +12.1 mV and +15.4 mV, respectively (Table 1), implying that both of them were stable colloidal nanoparticles.

Additional CD measurements confirmed that even after entrapping siRNA molecules, the AmPDs nanoassemblies still kept their secondary configuration (Fig. 3E). Following data analysis by CDNN software showed that the percentage of alpha-helical conformation of the siRNA/AmPDs complexes increased to ~30% (Table 1), which will be beneficial for subsequent intracellular uptake.

Further assessments of the cellular uptake of siRNA/AmPDs complexes were carried out with Cy5-labeled siRNA in human prostate cancer PC-3 cells and human ovarian cancer SKOV-3 cells using flow cytometry and confocal microscopy. Both Cy5-siRNA/$2C_{18}$-KK_2 and Cy5-siRNA/$2C_{18}$-KK_2K_4 complexes exhibited efficient uptake in PC-3 cells (Fig. 3F and H) and SKOV-3 cells (Fig. 3G and I). All the above findings demonstrated that the AmPDs were able to entrap siRNA to form stable nanoparticles, providing efficient protection of the resulting siRNA/AmPDs nanoparticles against enzymatic degradation and promoting their rapid and efficient intracellular uptake.

Safety assessment of AmPDs-mediated siRNA delivery systems

Before moving to examine the siRNA delivery and gene silencing mediated by AmPDs, we first assessed the safety of AmPDs-mediated siRNA delivery systems using 3-(4,5-dimethylthiazol-2-yl)-2,5-diphenyltetrazolium bromide (MTT) and lactate dehydrogenase (LDH) as well as hemolysis assays. MTT assays ascertain the metabolic toxicity by measuring cell viability, whereas LDH assays monitor the toxicity resulted from cell membrane damage by detecting LDH release in the cells. Results from MTT assays in both cancer cells (prostate cancer PC-3 cells and ovarian cancer SKOV-3 cells) and normal cells (human embryonic kidney HEK293 cells and mouse fibroblast L929 cells) showed no significant inhibition on cell growth after treating with siRNA/$2C_{18}$-KK_2 and siRNA/$2C_{18}$-KK_2K_4 complexes (Fig. 4A and B). Meanwhile, neither siRNA/$2C_{18}$-KK_2 nor siRNA/$2C_{18}$-KK_2K_4 induced, obviously, LDH release in those cell lines (Fig. 4C and D). The results from the above two studies indicated that siRNA/AmPDs complexes did not induce notable metabolic toxicity and cell membrane damages under the conditions for siRNA delivery. Moreover, the results of hemolysis assays confirmed that neither siRNA/$2C_{18}$-KK_2 nor siRNA/$2C_{18}$-KK_2K_4 exhibited hemolytic toxicity (Fig. 4E). All the results suggest that AmPDs-based siRNA delivery systems have non-toxic characteristics.

Different performance of AmPDs for siRNA delivery and the rationale behind

Encouraged by the promising cell uptake and safety profile of AmPDs-based delivery systems, we investigated their siRNA delivery capacity in prostate cancer PC-3 cells and ovarian cancer SKOV-3 cells. The siRNA molecules used in this study were designed to target either heat shock protein 27 (Hsp27) or protein kinase B (AKT2), both of which are oncogenes related to cell survival and apoptosis, and have been considered as promising therapeutic targets in cancer treatments (Rocchi *et al*. 2004; Testa and Bellacosa 2001). As shown in Fig. 5A and B, the expression of Hsp27 and AKT2 proteins was attenuated effectively after the treatment with siRNA/$2C_{18}$-KK_2K_4 complexes in PC-3 cells and SKOV-3 cells, whereas siRNA/$2C_{18}$-KK_2 complexes did not induce evident silencing of Hsp27 and AKT2. This finding indicated that $2C_{18}$-KK_2K_4 featuring bigger hydrophilic dendron delivered siRNA more effectively than $2C_{18}$-KK_2 bearing smaller dendron.

Next, we performed investigations to explore the underlying rationale of the different performance of AmPDs in siRNA delivery and gene silencing. Since the siRNA/$2C_{18}$-KK_2 and siRNA/$2C_{18}$-KK_2K_4 complexes showed similar cellular uptake in both these two cell lines (Fig. 3F and G), we hypothesized that the siRNA release process might be more efficient for siRNA/$2C_{18}$-KK_2K_4 than for siRNA/$2C_{18}$-KK_2, as efficient siRNA release also plays a very important role for the ultimate gene silencing effect. In order to validate this

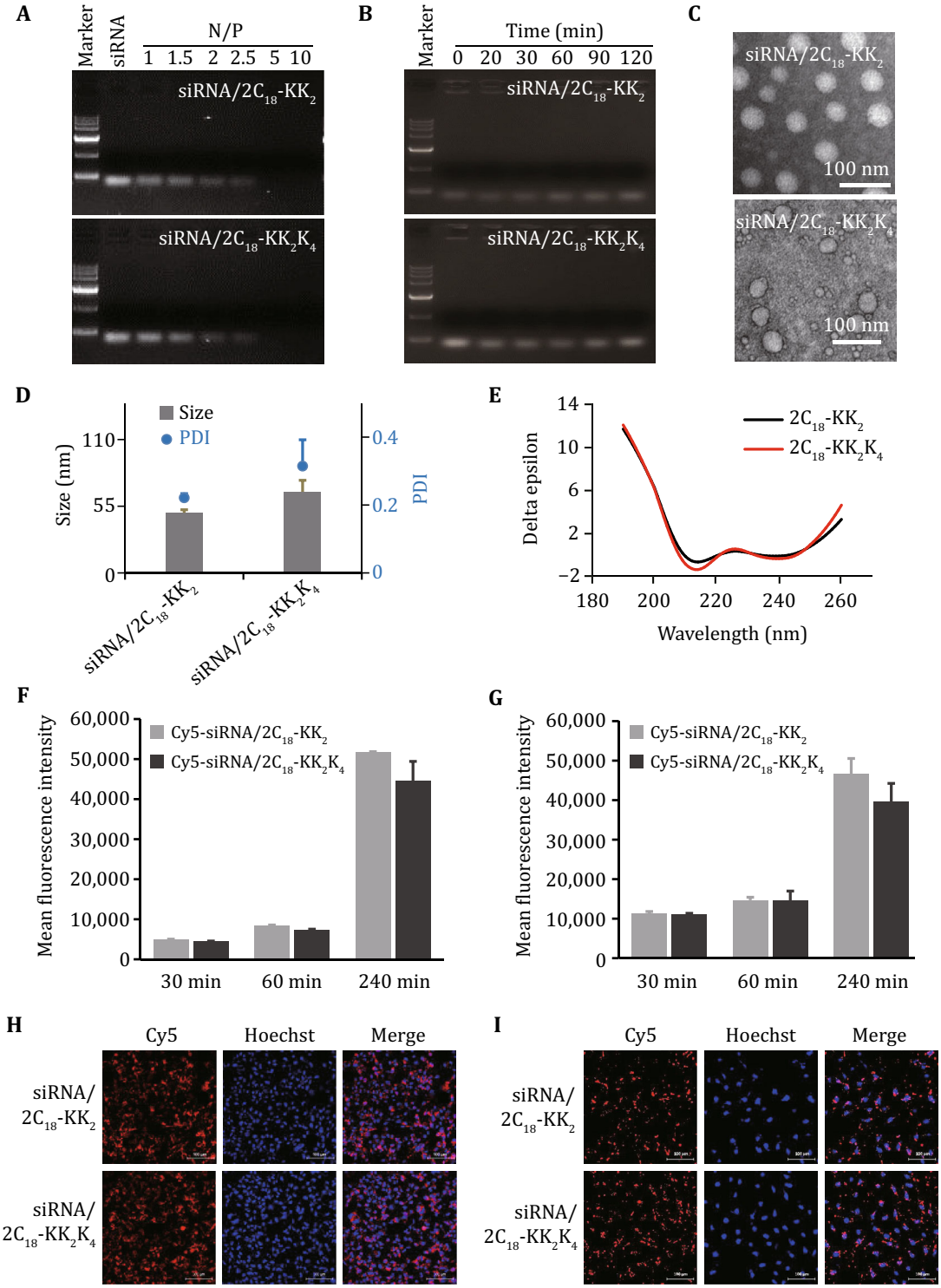

Fig. 3 Characterization of siRNA/AmPDs complexes. **A** Gel retardation assay of siRNA with AmPDs at N/P ratios ranging from 1 to 10. **B** Agarose gel retardation of siRNA/AmPDs complexes incubated with RNase A and SDS at different time (N/P ratio of 10). **C**, **D** TEM images (**C**) and DLS analysis (**D**) of the siRNA/AmPDs complexes (N/P ratio of 10). **E** CD spectrum of siRNA/AmPDs complexes at concentrations of 0.50 mg/mL in H_2O. **F**, **G** Flow cytometry analysis of the cell internalization of siRNA/AmPDs complexes (50 nmol/L Cy5-labeled siRNA, N/P ratio of 10) on PC-3 cells (**F**) and SKOV-3 cells (**G**). **H**, **I** Confocal microscopy images of the cell internalization of siRNA/AmPDs complexes (50 nmol/L Cy5-labeled siRNA, N/P ratio of 10) on PC-3 cells (**H**) and SKOV-3 cells (**I**). Red channel image shows the Cy5-labeled siRNA/AmPDs complexes (red), and blue channel image shows the nuclei of cells stained by Hoechst33342 (blue). Scale bars, 100 μm

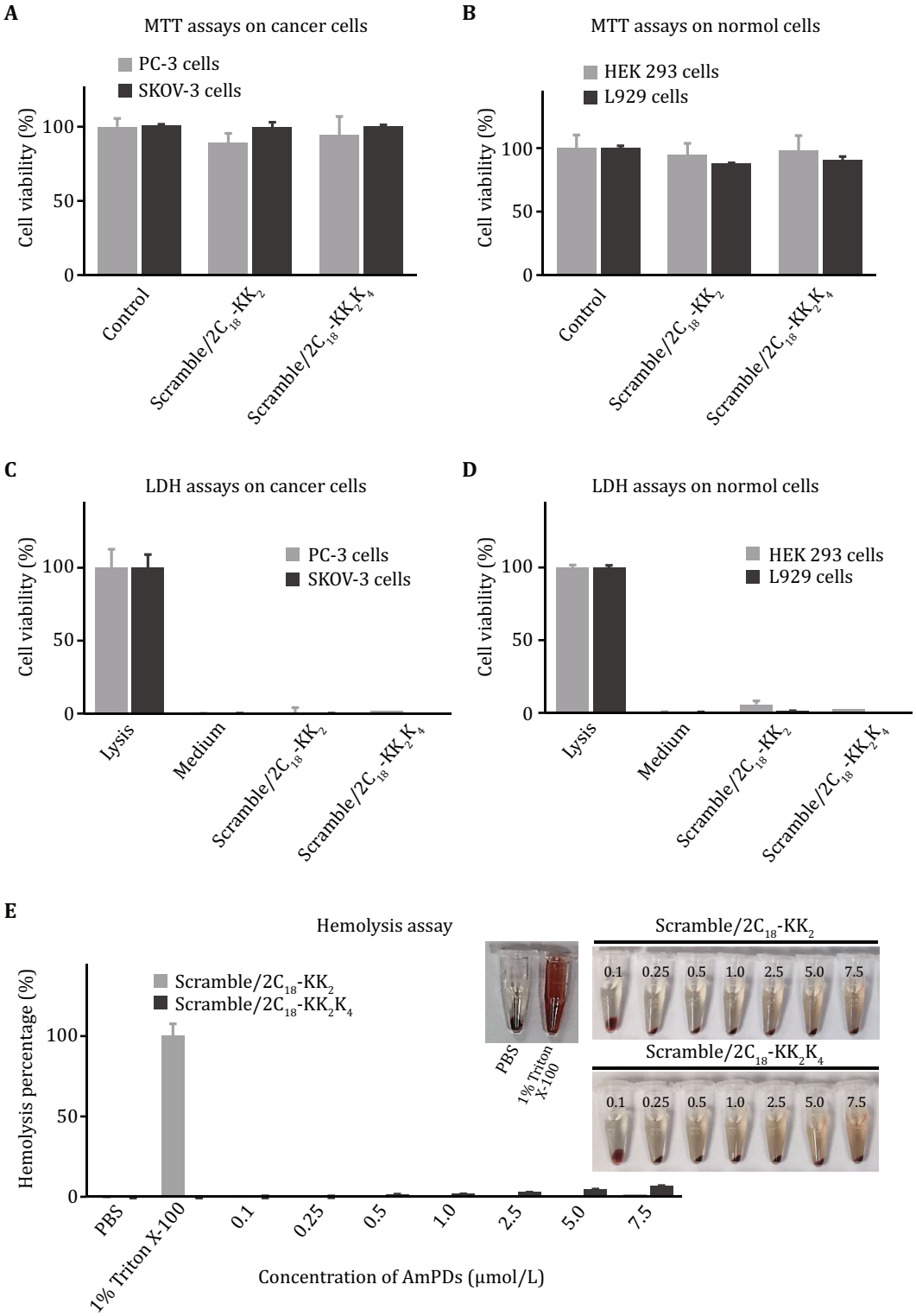

Fig. 4 Safety assessment of siRNA/AmPDs complexes. **A**, **B** The assessment of metabolic toxicity by MTT assay on cancer cells (PC-3 cells and SKOV-3 cells) (**A**) and normal cells (HEK293 cells and L929 cells) (50 nmol/L scramble siRNA, N/P ratio of 10) (**B**). mean ± SD, n = 3. **C**, **D** The assessment of cell membrane damage by LDH assay on cancer cells (PC-3 cells and SKOV-3 cells) (**C**) and normal cells (HEK293 cells and L929 cells) (50 nmol/L scramble siRNA, N/P ratio of 10) (**D**). mean ± SD, n = 3. **E** Hemolysis assay of the scramble/AmPDs complexes at varying concentrations from 0.1 to 7.5 μmol/L (N/P ratio of 10). mean ± SD, n = 3

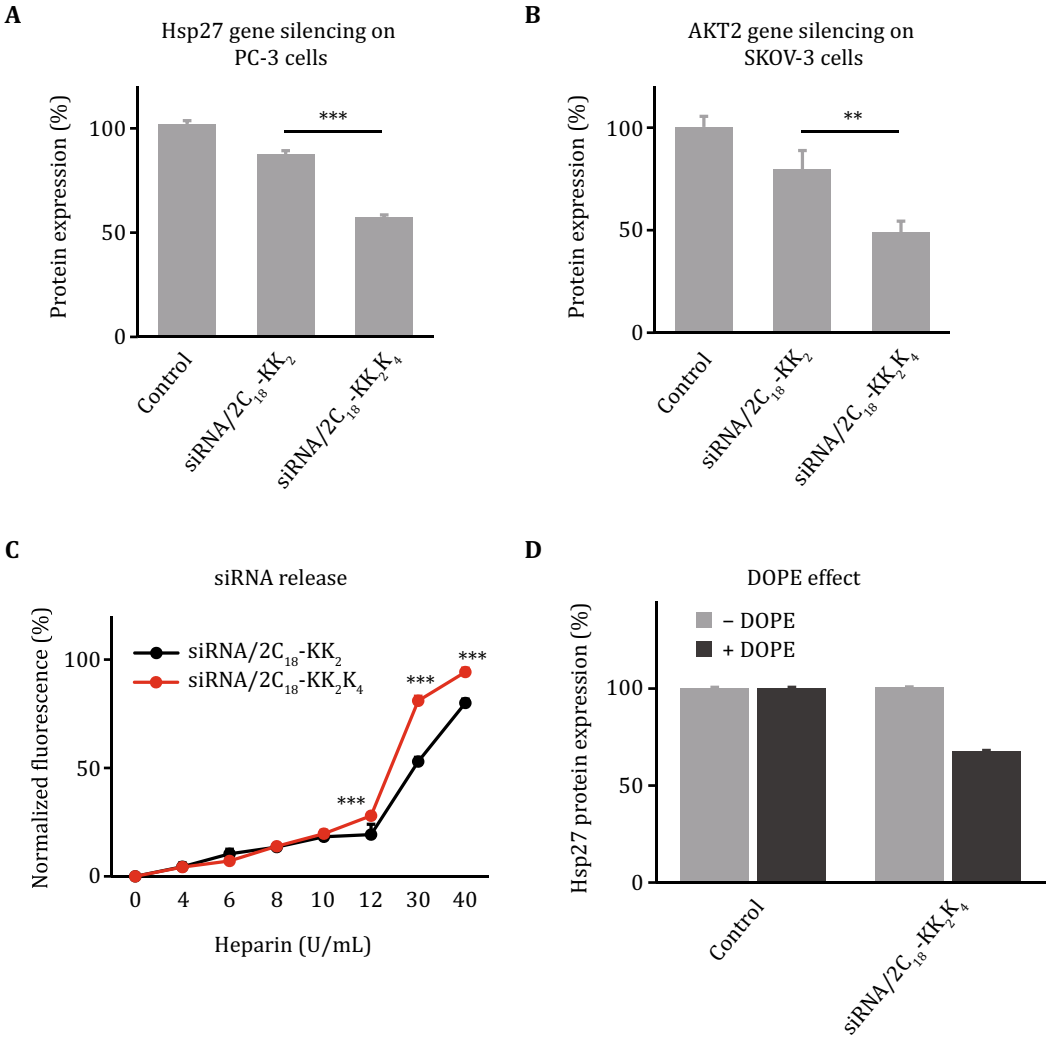

Fig. 5 Different performance of AmPDs for functional siRNA delivery and the underlying rationale. **A**, **B** Hsp27 protein expression on PC-3 cells (**A**) and AKT2 protein expression on SKOV-3 cells (**B**) after treatment with siRNA/AmPDs complexes quantified by Western blotting (50 nmol/L siRNA, N/P ratio of 10). $^{**}p \leq 0.01$, $^{***}p \leq 0.001$. mean ± SD, $n = 3$. **C** siRNA release from the siRNA/AmPDs complexes were determined by heparin replacement assay. $^{***}p \leq 0.001$. mean ± SD, $n = 3$. **D** Dioleoylphosphatidylethanolamine (DOPE) enhanced the gene silencing of Hsp27 after treatment of siRNA/$2C_{18}$-KK_2K_4 complexes with 20 nmol/L siRNA at N/P ratio 10 on PC-3 cells. mean ± SD, $n = 3$

speculation, we used heparin replacement assay to study the siRNA dissociation from the corresponding siRNA/AmPDs complexes at pH 5.0, which mimics the acidic environment of the endosome. Heparin is a kind of negatively charged polysaccharide that is frequently employed to compete with siRNA for binding to cationic vectors. As showed in Fig. 5C, with the increasing of heparin concentration, the siRNA molecules were displaced more effectively from siRNA/$2C_{18}$-KK_2K_4 complexes than from siRNA/$2C_{18}$-KK_2 complexes. This finding is in accordance with our hypothesis: $2C_{18}$-KK_2K_4 are indeed endowed with better siRNA releasing ability than $2C_{18}$-KK_2. This may be attributed to AmPD $2C_{18}$-KK_2K_4 possessing a good balance between hydrophobic portion and hydrophilic dendron generations, providing it with idea features to self-assemble into supramolecular nanoassemblies with optimal siRNA binding strength. Such nanovehicles are able to form stable complexes with siRNA, but more ready to disassemble during endosome escape, ultimately leading to better siRNA delivery and more potent silence than AmPD $2C_{18}$-KK_2.

Furthermore, we studied the gene silencing of siRNA/$2C_{18}$-KK_2K_4 complexes in the presence of the fusogenic lipid dioleoylphosphatidylethanolamine (DOPE) to corroborate that the good delivery capability of $2C_{18}$-KK_2K_4

is also benefited from the advantages of lipid vectors. DOPE is a kind of fusogenic lipid, which can usually be harnessed to improve the delivery capacity of lipid vehicles. In line with our expectation, the gene silencing efficiency of siRNA/$2C_{18}$-KK_2K_4 complexes was significantly enhanced in the presence of DOPE, implying the lipid-vector-like features of $2C_{18}$-KK_2K_4 (Fig. 5D). This finding, together with the protein-mimic properties of $2C_{18}$-KK_2K_4 observed by CD analysis, suggested that the AmPD $2C_{18}$-KK_2K_4 indeed combines the advantages of both lipid and peptide dendrimer vectors.

CONCLUSIONS

In this study, we developed novel amphiphilic peptide dendrimers (AmPDs), composed of hydrophobic two C_{18} alkyl chains and hydrophilic poly(lysine) dendrons of different generations ($2C_{18}$-KK_2 and $2C_{18}$-KK_2K_4), as safe and efficient nanovehicles for functional siRNA delivery. Our studies revealed that AmPDs were able to self-assemble into supramolecular nanoassemblies, form stable complexes with siRNA, protect siRNA from enzymatic degradation, and facilitate efficient cell uptake of siRNA without notable toxicity. Further investigations demonstrated that, compared with AmPD $2C_{18}$-KK_2 bearing smaller dendrons, AmPD $2C_{18}$-KK_2K_4 bearing bigger generation of hydrophilic dendrons was able to entrap siRNA to form stable but more ready to disassemble nanoparticles by virtue of its optimal balance between hydrophobic lipid-like portion and hydrophilic poly(lysine) dendron generations, therefore resulting in better performance on releasing of siRNA molecules and silencing targeted genes. Our findings open a new perspective on the design of self-assembly amphiphilic dendrimers for functional and adaptive delivery of siRNA therapeutics.

MATERIALS AND METHODS

Synthesis and characterization of AmPDs

The detailed synthetic processes and characterization data of AmPDs can be found in the Supplementary materials.

Materials

The human Hsp27 siRNA, AKT2 siRNA, scramble siRNA, and Cy5-siRNA were purchased from Guangzhou Ruibo (Guangzhou, China). All the other reagents and solvents were used without any further purification from commercial sources.

Critical aggregation concentration (CAC) values

CAC of AmPDs was determined using 2.5×10^{-6} mol/L Nile Red as a fluorescence probe. After ultrasonic treatment for 30 min, solution rests at room temperature for 2 h, and then Cytation5 (BioTek, Vermont, USA) is to detect the solution. The excitation wavelength and emission wavelengths were 550 nm and 650 nm, respectively.

Dynamic light scattering (DLS)

siRNA solution or H_2O were mixed with AmPDs solution in H_2O. The solution was incubated for 30 min, and then size distribution and zeta potential measurement of the solution were performed using NanoBrookOmni (Brookhaven, Long Island, N.Y.).

Transmission electronic microscopy (TEM)

The solution of siRNA was mixed with AmPDs solution in H_2O and incubated for 30 min. The dried complexes were inspected in a transmission electron microscope (TEM) operated at 100 kV (HT7700).

Circular dichroism (CD) analysis

The CD experiments were executed on the Chirascan spectrometer (Applied Photophysics Ltd., Leatherhead, UK) by using CDNN software to analyze the data. The concentration of AmPDs samples in water was 0.50 mg/mL.

Gel retardation analysis

The siRNA solution was mixed with AmPDs solution in H_2O at N/P ratios from 1/1 to 10/1 and then incubated the siRNA/AmPDs complexes at room temperature for 30 min. The complexes were mixed with 6× loading buffer and then shifted in 1% agarose gel which is stained by GoodView^{TM} (Solarbio) in standard 1× TAE buffer. The results were detected by a Tanon CCD camera (type 2500) (Tanon, Shanghai, China).

RNase A assay

siRNA (200 ng/well) and AmPDs with N/P ratio 10 were kept at room temperature for 30 min, and then the complexes were incubated with RNase A (0.25 μg/mL) at 37 °C for different times and then treated with 1%

SDS solution at 4 °C. Then, samples were run in a 1% agarose gel and then detected by a Tanon CCD camera (type 2500) (Tanon, Shanghai, China). Naked siRNA was used as a control.

RNA dissociation assay

Ethidium bromide and siRNA were incubated in 1× PBS buffer (pH 5.0) for 10 min. Then AmPDs solution with N/P ratio 10 and additional PBS (or PBS alone) were added into those siRNA solutions and the complex was incubated for 30 min. Heparin with different concentrations diluted in PBS was mixed with siRNA complexes to incubate for another 30 min. And then the mixture was excited at 360 nm and recorded at 590 nm using Cytation5 (BioTek, Vermont, USA). All samples were repeated in triplicate.

Cell culture

Human prostate cancer PC-3 cells were cultured in HyClone^{TM} DMEM (GE, Logan. UT. USA) containing 10% Gibco^{TM} fetal bovine serum (FBS) (Thermo Fisher SCIENTIFIC, Carlsbad, CA, USA). Human ovarian cancer SKOV-3 cells were cultured in McCOY'S 5A (Hyclone, USA) with 10% FBS. Human embryonic kidney HEK293 cells were maintained in MEM (Hyclone, USA) with 10% FBS. Mouse fibroblast L929 cells were cultured in RPMI-1640 (Hyclone, USA) with 10% FBS. All cells were cultured in an incubator with a humidified environment of 5% CO_2 and a constant temperature of 37 °C.

Cellular uptake

Flow cytometry

24 h before transfection, PC-3 cells and SKOV-3 cells (5×10^4) were seeded into 24-well plates and then incubated with Cy5-siRNA/AmPDs complex (50 nmol/L Cy5-siRNA, N/P ratio 10) at 37 °C. The cells were washed with PBS and collected to analyze by the Attune NxT acoustic focusing cytometer (Thermo Fisher SCIENTIFIC, Carlsbad, CA, USA).

Confocal microscopy

PC-3 cells and SKOV-3 cells (1×10^5) were seeded in confocal plates (NEST, China) and grown for 24 h, and then the cells were incubated with Cy5-siRNA/AmPDs complex (50 nmol/L Cy5-siRNA, N/P ratio 10) for 8 h at 37 °C and stained with Hoechst33342 and Lyso Tracker Red for 15 min at 37 °C. A Zeiss LSM880 Meta laser scanning confocal microscope (Carl Zeiss, Jena, Germany) was used for visualization, utilizing ZEN2.3 pro software (Carl Zeiss GmbH) to acquire images.

In vitro transfection

Cancer cells (1×10^5) were seeded in 6-well plates and grown for 24 h. The solutions of Hsp27 siRNA/AmPDs complexes (50 nmol/L siRNA, N/P ratio 10) or AKT2 siRNA/AmPDs complexes were prepared before transfection. After transfected for 8 h, the transfection mixture was replaced with the complete medium and cells were incubated for an additional 72 h for Western blot assay.

MTT (3-(4,5-dimethylthiazol-2-yl)-2,5-diphenyl tetrazolium bromide) assay

Cancer cells (SKOV-3 cells and PC-3 cells) and normal cells (HEK293 cells and L929 cells) (5×10^3) were seeded in 96-well plates and cultured for 24 h. Cells were then treated with siRNA/AmPDs (50 nmol/L siRNA, N/P ratio 10) for 8 h. After transfection, the medium was replaced with fresh medium. 24 h later, the cells were treated with MTT solution and incubated for another four hours. After removing the solution, the cells were re-suspended in DMSO. The optical density (OD) of DMSO solutions was read at 570 nm via Cytation5 (BioTek, Vermont, USA). The difference between the OD values of the treated and non-treated cells reflects the viability of cells after treatment and, thus, represents the metabolic toxicity. All samples were repeated in triplicate.

Lactate dehydrogenase (LDH) assay

Cancer cells (SKOV-3 cells and PC-3 cells) and normal cells (HEK293 cells and L929 cells) were treated with siRNA/AmPDs complex. After 24 h, we used a commercial LDH kit (Cytotoxicity Detection Kit, Roche) to measure the LDH concentration, and the LDH reaction mixture was freshly prepared according to the manufacturer's protocol (Roche Diagnostics). Control was performed with lysis buffer and medium and set as 100% and 0% LDH release, respectively.

Hemolysis experiment

Red blood cells (RBCs) were isolated from mice blood and diluted to achieve a solution with a concentration of 2%. The RBC solution was added into siRNA/AmPDs. PBS or 1% TritonX-100 (Beyotime Biotechnology, Shanghai, China) solution was used as the negative control and positive control, respectively. The samples

were left at 37 °C for 2 h and then centrifuged. The absorbance of hemoglobin at 540 nm was measured. Each assay was performed in triplicate.

Acknowledgements This work was financially supported by the Key Program for International S&T Cooperation Projects of China (2018YFE0117800), the National Natural Science Foundation of China (51773227, 81701815), Natural Science Foundation of Jiangsu Province (BK20170735), the Youth Thousand-Talents Program of China, the Program for Jiangsu Province Innovative Research Talents, the Program for Jiangsu Province Innovative Research Team, the State Key Laboratory of Natural Medicines at China Pharmaceutical University (SKLNMZZ202007), and "Double First-Class" project of China Pharmaceutical University (CPU2018GF05).

Compliance with Ethical Standards

Conflict of interest Chi Ma, Dandan Zhu, Yu Chen, Yiwen Dong, Wenyi Lin, Ning Li, Wenjie Zhang, and Xiaoxuan Liu declare that they have no conflict of interest.

Human and animal rights and informed consent This article does not contain any studies with human or animal subjects performed by any of the authors.

References

(2020) Second RNAi drug approved. Nat Biotechnol 38: 385

Bajan S, Hutvagner G (2020) RNA-based therapeutics: from antisense oligonucleotides to miRNAs. Cells 9(1):137. https://doi.org/10.3390/cells9010137

Bracci L, Falciani C, Lelli B, Lozzi L, Runci Y, Pini A, De Montis MG, Tagliamonte A, Neri P (2003) Synthetic peptides in the form of dendrimers become resistant to protease activity. J Biol Chem 278(47):46590–46595

Castanotto D, Rossi JJ (2009) The promises and pitfalls of RNA-interference-based therapeutics. Nature 457(7228):426–433

Chen C, Posocco P, Liu X, Cheng Q, Laurini E, Zhou J, Liu C, Wang Y, Tang J, Col VD, Yu T, Giorgio S, Fermeglia M, Qu F, Liang Z, Rossi JJ, Liu M, Rocchi P, Pricl S, Peng L (2016) Mastering dendrimer self-assembly for efficient siRNA delivery: from conceptual design to *in vivo* efficient gene silencing. Small 12(27):3667–3676

Crespo L, Sanclimens G, Pons M, Giralt E, Royo M, Albericio F (2005) Peptide and amide bond-containing dendrimers. Chem Rev 105(5):1663–1681

Darbre T, Reymond JL (2006) Peptide dendrimers as artificial enzymes, receptors, and drug-delivery agents. Acc Chem Res 39(12):925–934

Dong Y, Chen Y, Zhu D, Shi K, Ma C, Zhang W, Rocchi P, Jiang L, Liu X (2020) Self-assembly of amphiphilic phospholipid peptide dendrimer-based nanovectors for effective delivery of siRNA therapeutics in prostate cancer therapy. J Control Release 322:416–425

Dong Y, Yu T, Ding L, Laurini E, Huang Y, Zhang M, Weng Y, Lin S, Chen P, Marson D, Jiang Y, Giorgio S, Pricl S, Liu X, Rocchi P, Peng L (2018) A dual targeting dendrimer-mediated siRNA delivery system for effective gene silencing in cancer therapy. J Am Chem Soc 140(47):16264–16274

Heitz M, Javor S, Darbre T, Reymond JL (2019) Stereoselective pH responsive peptide dendrimers for siRNA transfection. Bioconjug Chem 30(8):2165–2182

Inoue Y, Kurihara R, Tsuchida A, Hasegawa M, Nagashima T, Mori T, Niidome T, Katayama Y, Okitsu O (2008) Efficient delivery of siRNA using dendritic poly(L-lysine) for loss-of-function analysis. J Control Release 126(1):59–66

Juliano RL (2016) The delivery of therapeutic oligonucleotides. Nucleic Acids Res 44(14):6518–6548

Kanasty R, Dorkin JR, Vegas A, Anderson D (2013) Delivery materials for siRNA therapeutics. Nat Mater 12(11):967–977

Kay RF (2015) Drugging RNAi. Science 347(6226):1068–1069

Kesharwani P, Jain K, Jain NK (2014) Dendrimer as nanocarrier for drug delivery. Prog Polym Sci 39(2):268–307

Khandare J, Calderon M, Dagia NM, Haag R (2012) Multifunctional dendritic polymers in nanomedicine: opportunities and challenges. Chem Soc Rev 41(7):2824–2848

Kim B, Park JH, Sailor MJ (2019) Rekindling RNAi therapy: materials design requirements for *in vivo* siRNA delivery. Adv Mater 31(49):e1903637. https://doi.org/10.1002/adma.201903637

Ledford H (2018) Gene-silencing technology gets first drug approval after 20-year wait. Nature 560(7718):291–292

Lee CC, MacKay JA, Frechet JM, Szoka FC (2005) Designing dendrimers for biological applications. Nat Biotechnol 23(12):1517–1526

Li Y, Bai H, Wang H, Shen Y, Tang G, Ping Y (2018) Reactive oxygen species (ROS)-responsive nanomedicine for RNAi-based cancer therapy. Nanoscale 10(1):203–214

Liu X, Liu C, Zhou J, Chen C, Qu F, Rossi JJ, Rocchi P, Peng L (2015) Promoting siRNA delivery via enhanced cellular uptake using an arginine-decorated amphiphilic dendrimer. Nanoscale 7(9):3867–3875

Liu X, Wang Y, Chen C, Tintaru A, Cao Y, Liu J, Ziarelli F, Tang J, Guo H, Rosas R, Giorgio S, Charles L, Rocchi P, Peng L (2016) A fluorinated bola-amphiphilic dendrimer for on-demand delivery of siRNA, via specific response to reactive oxygen species. Adv Func Mater 26(47):8594–8603

Liu X, Zhou J, Yu T, Chen C, Cheng Q, Sengupta K, Huang Y, Li H, Liu C, Wang Y, Posocco P, Wang M, Cui Q, Giorgio S, Fermeglia M, Qu F, Pricl S, Shi Y, Liang Z, Rocchi P, Rossi JJ, Peng L (2014) Adaptive amphiphilic dendrimer-based nanoassemblies as robust and versatile siRNA delivery systems. Angew Chem Int Ed Engl 53(44):11822–11827

Luo K, Li C, Li L, She W, Wang G, Gu Z (2012) Arginine functionalized peptide dendrimers as potential gene delivery vehicles. Biomaterials 33(19):4917–4927

Malhotra S, Bauer H, Tschiche A, Staedtler AM, Mohr A, Calderon M, Parmar VS, Hoeke L, Sharbati S, Einspanier R, Haag R (2012) Glycine-terminated dendritic amphiphiles for nonviral gene delivery. Biomacromol 13(10):3087–3098

Mintzer MA, Grinstaff MW (2011) Biomedical applications of dendrimers: a tutorial. Chem Soc Rev 40(1):173–190

Mullard A (2020) RNAi agents score an approval and drive an acquisition. Nat Rev Drug Discov 19(1):10–10

Ozpolat B, Sood AK, Lopez-Berestein G (2014) Liposomal siRNA nanocarriers for cancer therapy. Adv Drug Deliv Rev 66:110–116

Percec V, Wilson DA, Leowanawat P, Wilson CJ, Hughes AD, Kaucher MS, Hammer DA, Levine DH, Kim AJ, Bates FS, Davis KP, Lodge TP, Klein ML, DeVane RH, Aqad E, Rosen BM, Argintaru AO, Sienkowska MJ, Rissanen K, Nummelin S, Ropponen J (2010) Self-assembly of Janus dendrimers into uniform dendrimersomes and other complex architectures. Science 328(5981):1009–1014

Rocchi P, So A, Kojima S, Signaevsky M, Beraldi E, Fazli L, Hurtado-Coll A, Yamanaka K, Gleave M (2004) Heat shock protein 27 increases after androgen ablation and plays a cytoprotective role in hormone-refractory prostate cancer. Cancer Res 64(18):6595–6602

Sadler K, Tam JP (2002) Peptide dendrimers: applications and synthesis. J Biotechnol 90(3–4):195–229

Sapra R, Verma RP, Maurya GP, Dhawan S, Babu J, Haridas V (2019) Designer peptide and protein dendrimers: a cross-sectional analysis. Chem Rev 119(21):11391–11441

Setten RL, Rossi JJ, Han SP (2019) The current state and future directions of RNAi-based therapeutics. Nat Rev Drug Discov 18(6):421–446

Svenson S, Tomalia D (2005) Dendrimers in biomedical applications—reflections on the field. Adv Drug Deliv Rev 57(15):2106–2129

Testa JR, Bellacosa A (2001) AKT plays a central role in tumorigenesis. Proc Natl Acad Sci USA 98(20):10983–10985

Wagner E (2012) Polymers for siRNA delivery: inspired by viruses to be targeted, dynamic, and precise. Acc Chem Res 45(7):1005–1013

Weng Y, Xiao H, Zhang J, Liang X-J, Huang Y (2019) RNAi therapeutic and its innovative biotechnological evolution. Biotechnol Adv 37(5):801–825

Whitehead KA, Langer R, Anderson DG (2009) Knocking down barriers: advances in siRNA delivery. Nat Rev Drug Discov 8(2):129–138

Wittrup A, Lieberman J (2015) Knocking down disease: a progress report on siRNA therapeutics. Nat Rev Genet 16(9):543–552

Wu M, Liu X, Jin W, Li Y, Li Y, Hu Q, Chu PK, Tang G, Ping Y (2017) Targeting ETS1 with RNAi-based supramolecular nanoassemblies for multidrug-resistant breast cancer therapy. J Control Release 253:110–121

Yin H, Kanasty RL, Eltoukhy AA, Vegas AJ, Dorkin JR, Anderson DG (2014) Non-viral vectors for gene-based therapy. Nat Rev Genet 15(8):541–555

Yu T, Liu X, Bolcato-Bellemin AL, Wang Y, Liu C, Erbacher P, Qu F, Rocchi P, Behr JP, Peng L (2012) An amphiphilic dendrimer for effective delivery of small interfering RNA and gene silencing *in vitro* and *in vivo*. Angew Chem Int Ed Engl 51(34):8478–8484